Presented at the 17th International Conference on Indoor Air Quality and Climate, Indoor Air 2022; Reprinted with friendly permission from ISIAQ

Impact of Non-Occupied Seats on the Thermal Comfort in Long-Range Aircraft for Novel Ventilation Concepts

Tobias Dehne* [1], Pascal Lange[1], Daniel Schmeling[1], Ingo Gores[2]

[1] German Aerospace Center (DLR), Institute of Aerodynamics and Flow Technology, Bunsenstraße 10, 37073 Göttingen, Germany
[2] Airbus Operations GmbH, Kreetslag 10, 21129 Hamburg, Germany

*Corresponding email: tobias.dehne@dlr.de

SUMMARY
The performance of the aircraft cabin ventilation system for not fully occupied cabins, is an important evaluation parameter. Low-Momentum Ceiling Ventilation (LMCV), a novel ventilation concept for aircraft cabins, was experimentally investigated under static flight conditions in a full-scale twin aisle cabin mock-up within the scope of the Clean-Sky 2 Joint Undertaking project ADVENT. The usage of a jacket cooling system and of temperature controlled thermal manikins ensured the simulation of realistic boundary conditions. Three different cases of incompletely occupied cabins with adapted volume flow rates are compared to a completely filled cabin. Main finding is that a reduction of the volume flow rate by up to 40% can maintain comfortable conditions for reduced passenger load. However, the results also highlighted the increased risk of non-desired bypass flows for increased supply air temperatures. The latter were a direct result to maintain the mean cabin temperature at a comfortable level.

KEYWORDS
Long-Range Aircraft Cabin Ventilation, Thermal Passenger Comfort, Novel Ventilation Concepts, Passenger Load Factor

1 INTRODUCTION
Novel ventilation systems for aircraft cabins have attracted the attention of scientists and aircraft manufacturers during the last years. According to IATA (2009), the global fleet's CO2 emission rate should be reduced by 50% until 2050 desiring technical innovations in all components of an aircraft. Further, up to 75% of non-propulsive power is used by the Environmental Control System (ECS) for conditioning of a passenger aircraft under normal cruise flight conditions Martinez (2014). With a general trend of rising heat loads in modern passenger cabins, the interest of the aircraft industry in the numerical as well as experimental investigation of novel ventilation systems is of high importance. Previous studies deal with cabin displacement ventilation (CDV) (Yin et al. (2007), Schmidt (2008), Zhang et al. (2009)), where the fresh air is supplied with small momentum. At the German Aerospace Center (DLR), high heat removal efficiencies and low draft rates were discovered for CDV as compared to the state-of-the-art mixing ventilation in grounded (Bosbach et al. (2013)) as well as flight tests (Bosbach et al. (2012)). A multi-zonal temperature control system of transient thermal loads in mixing ventilation of passenger aircraft cabins was developed and investigated with seven different heat load scenarios by Dehne et al. (2018). Averaged over all load scenarios, the baseline case yielded 14% of seats with temperature deviations larger than 0.5 K from the column mean. By switching to a multi-zonal control, the value was reduced by almost one order of magnitude to 1.6%.

To allow for a greener and smarter testing of novel ventilation concepts for future long-range airliners, a full-scale twin aisle cabin mock-up with thermodynamically realistic boundary conditions by means of temperature-controlled fuselage elements was developed at the German Aerospace Center (DLR) in Göttingen, see Lange et al. (2020). The modular construction of the new facility allows the installation of different cabin geometries while simultaneously providing a high flexibility for the integration of novel ventilation concepts. Beside the normal flight condition "cruise", the "Hot-Day-on-Ground" scenario, representing all ground movements of an aircraft at very warm ambient temperatures, was investigated with a 50%-50% volume flow split rate between straight and inclined outlets, highlighting the capabilities of the new research facility. Six modifications of Micro-Jet Ventilation (MJV) with different air inlet configurations were analysed in Dehne et al. (2022) focussing at optimal parameters for thermal comfort as well as energy saving. The study revealed almost optimal comfort parameters for two MJV configurations for future aircraft cabins. In an extended study, Lange et al. (2022) compared MJV to LMCV experimentally under two different thermodynamic boundary conditions representing different operational flight phases. Here, both concepts performed similar characterized by overall thermally comfortable conditions with slightly increased thermal passenger comfort and energy efficiency rating under warmer ambient conditions.
In this study, LMCV is investigated experimentally with regard to incompletely occupied cabins in the new full-scale, long-range aircraft cabin mock-up. Incompletely occupied cabins are rather the rule than the exception (typical passenger load factor is 75 to 90%, (IATA (2009)), and even much less during pandemic times). Changes of the horizontal temperature distribution by switching off thermal manikins on selected seats are investigated experimentally under realistic boundary conditions for the flight phase "cruise", which is characterized by cold temperature boundary conditions. To determine an energy saving potential, the volume flows are adjusted to compensate the missing passengers. The present work is of great importance for future comparisons with the reference case of state-of-the-art mixing ventilation (MV) as well as other novel ventilation systems and to determine the applicability of LMCV under non-optimal conditions.

2 MATERIALS/METHODS

With the aim to investigate LMCV in a realistic measurement environment, a full-scale cabin mock-up was developed and constructed at the German Aerospace Center (DLR) in Göttingen (Lange et al. (2020)). LMCV is characterized by a low-momentum air supply through planar and large-surface inlets, which are similarly aligned in the ceiling area with two inclined as well as two straight inlets in cross section, see Figure 1 (left). With nine inlets in longitudinal direction, overall 36 air inlets were installed in the mock-up. The inlet area is made of fabric membranes which ensures a uniform outflow with low and homogeneous flow velocities. The exhaust openings are located at both sides of the cabin below the luggage compartments, i.e. lateral exhaust. Following the results in Dehne et al. (2022), a volume flow rate split of 50%-50% between straight and inclined inlets revealed the best results regarding thermal comfort for a fully occupied cabin und thus is chosen for this analysis as well. All studied cases with the corresponding boundary conditions, such as flow rate (Q_V) as well as temperature for supplied (T_{in}) and exhausted air (T_{out}) are summarized in Table 1.
To investigate LMCV under real flight conditions, a jacket heating/cooling based on capillary tubes was implemented in the structure of the cabin mock-up, see Lange et al. (2020). In the present study, we concentrate on the normal flight level "cruise" with gap (between primary and secondary insulation) temperatures of 11°C. As a note, the mean cabin temperature (T_{cab}) serves as a control temperature and was kept constant with a maximum deviation of 0.1 K during the state of equilibrium, reflecting the high precision of the temperature control system

in the new mock-up. To reach the setpoint and keep it constant, T_{in} was adjusted individually for each studied case.
The thermal manikins (TMs) (for more details visit Dehne et al. (2022)) were heated by external power supplies and operated with an automatic control of the heat release of the manikins. This depends on the mean temperature in the cabin based on a standard (EN13129, (2016)) which provides a realistic simulation of the human metabolism. For the acquisition of the temperatures in the complete cabin, resistance temperature detectors (RTDs) at chest height were installed in front of all TMs. Ten measurement racks with RTDs at four height levels were installed close to the TMs at a distance of 5 cm to evaluate temperature stratifications in row 4, see Figure 1 (left) and sensor rack SR1 in Figure 1 (right). Furthermore, SR2 in Figure 1b) shows the measurement position of combined fluid temperature and velocity probes (OVTPs) in row 6, arranged exactly as the RTDs in row 4. The flow velocities are important for two reasons: First, the velocity should be low enough to prevent excessive draft. Second, the large-scale flow patterns and the small-scale turbulence structure of the cabin flow govern mixing and heat exchange and thus determine macroscopic quantities, such as heat removal efficiency, temperature homogeneity and temperature stratifications. With an accuracy of 0.2 K for the temperature and 0.02 m/s for the velocity, the comfort-relevant air velocities and their distribution for different body parts were recorded in row 6.

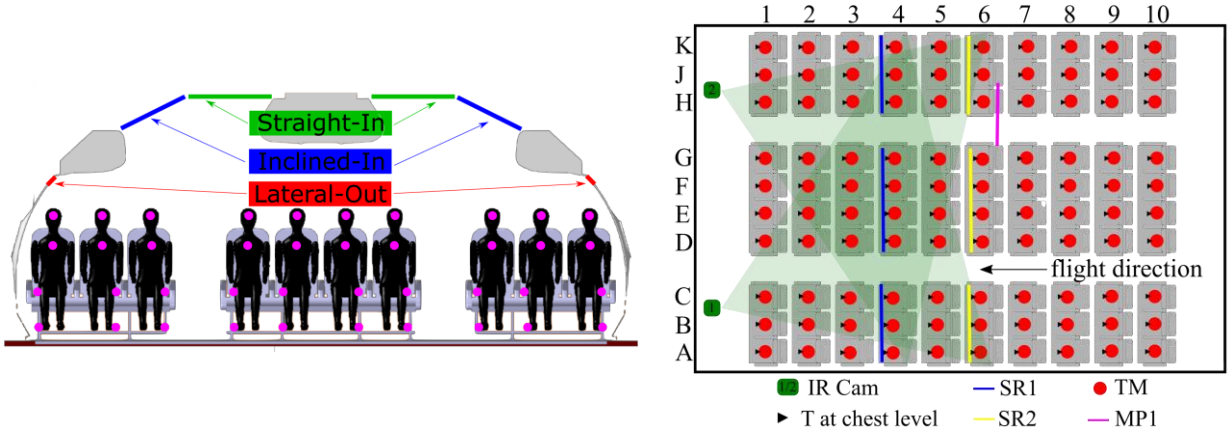

Figure 1. Left, sketch of Low-Momentum Ceiling Ventilation (LMCV) in the cabin mock-up with positioning of RTD and OVTP probes (magenta circles) near the TM at height level 0.05 m, 0.5 m, 0.95 m and 1.25 m mounted at SR1 and SR2 in seat row 4 and 6, respectively and right, cabin layout and measurement installation within the passenger compartment. SR1 and 2 denote the position of the sensor racks. MP1 depicts the measurement plane for the flow visualization. Further the positions of the infrared cameras are given.

Besides the fully occupied cabin (case 0), three dedicated heat load scenarios were realized by switching off TMs at different seat positions, marked in magenta in Figures 2a) – c) and listed in Table 1. In case 1, a checkerboard pattern was realized by switching off 50 TMs, see Figure 2a). Furthermore, only those TMs sitting at aisle and window seats were heated in case 2 (Figure 2b). This results in 40 switched off TMs. For case 3, a random pattern was designed with 30 switched off heat loads according to Figure 2c). Two infrared (IR) cameras were positioned in front of the first row (see Figure 1 right) to record the surface temperatures of the cabin and the manikins, see images in the top right corner in Figure 2 a) – c). Particularly in cases 1 and 2, the pattern of the switched-off heat loads is directly visible in the IR images. Pre-tests confirmed that the effect of switched-off vs. completely removed manikins is less than 0.2 K regarding the temperatures on the four height levels. Thus, it is concluded that computer-controlled deactivation of the manikins' heat release is suitable for the simulation of non-occupied seats. Two volume flows were investigated for all cases and listed in Table 1:

First, the “Norm Flow” case with 10 l/s/PAX = 1000 l/s, with PAX being the nominal seat capacity of 100 and second, the “Adapted Flow” with a volume flow adapted to the heat loads with 10 l/s/active TM.

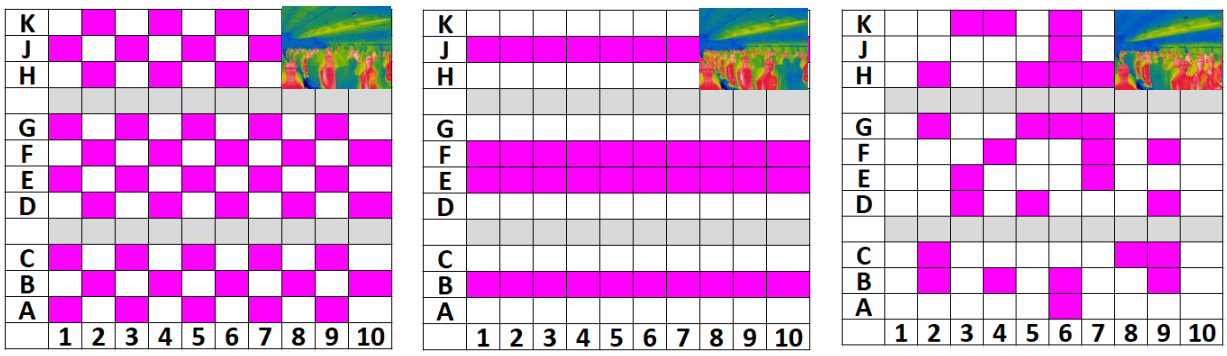

a) b) c)

Figure 2. Sketch of the investigated scenarios (a-c). Deactivated TMs, i.e. missing heat loads, are depicted in magenta. a) checkerboard pattern with 50% missing heat loads. b) free middle seats, i.e. 40% missing heat loads and c) random pattern with 30% missing heat loads. Infrared images of IR camera 2 corresponding to the investigated cases are shown in the top right corners.

As previously described, T_{in} was adjusted individually to reach the setpoint of a constant mean cabin temperature T_{cab}. We found that for each ten missing heat loads T_{in} has to increase by approximate 0.8 K at constant volume flow rates, see Table 1. Meanwhile, the temperature difference between T_{out} and T_{in} decreases by approximate 0.5 K per ten missing heat loads. The fact, that the temperatures of T_{in} and T_{out} are almost independent from the flow rate for the case with only 50% heat load is already a first indicator for a short-circuit flow discussed in section 3. An adjustment of T_{in} appears to be independent of the volume flow. As a result, the heat dissipation of the TMs does not take place via ventilation but via cold side walls. The exhaust temperature (T_{out}) also shows a temperature increase with increasing T_{in} at a constant T_{cab} and with reduced heat loads. Due to a constant temperature difference between T_{cab} and T_{gap}, the thermal energy dissipated through the side walls is also approximately constant, which means that the outflow temperature is higher for a higher number of heat loads.

Table 1. Boundary conditions for the investigated test cases with as flow rate (Q_V), temperature for supplied (T_{in}) and exhausted air (T_{out}), switched on TMs, $\Delta\langle T_{Chest}\rangle$ show the largest differences between maximum and minimum temperature at chest level with associated spatial standard deviation. Furthermore, $\Delta\langle T_{HA}\rangle$ reveals the maximum difference between temperatures at head and ankle also with associated standard deviation.

Case	Q_V^{in} [l/s]	T_{in} [°C]	T_{out} [°C]	TMs	$\Delta\langle T_{Chest}\rangle$ [K] all TMs	$\sigma\langle T_{Chest}\rangle$ [K] all TMs	$\Delta\langle T_{HA}\rangle$ [K] active TMs	$\sigma\langle T_{HA}\rangle$ [K] active TMs
C-0	1000	21.0	24.3	100	2.6	0.4	5.2	0.05
C-1.1	500	24.9	25.6	50	2.8	0.5	9.2	0.09
C-1.2	1000	24.8	25.3	50	2.8	0.5	8.7	0.07
C-2.1	600	23.4	25.3	60	2.9	0.5	8.3	0.10
C-2.2	1000	23.7	24.9	60	2.8	0.5	7.4	0.10
C-3.1	700	22.4	24.8	70	1.8	0.5	7.2	0.10
C-3.2	1000	22.9	24.5	70	1.9	0.5	6.7	0.09

3 RESULTS

Laser flow visualizations of the cabin air flow were created by emission of fog upstream to the cabin air inlets in measurement plane MP1, see Figure 1 (right). Figure 3 shows the resulting flow pattern for the reference C-0 as well as case 1 with adapted flow (C-1.1) and norm flow (C-1.2). For C-0 presented in Figure 3 a), the fresh supplied air is combined to a downwards flow in the aisle section between the lateral and centre luggage compartments. Subsequently, the fresh air moves first to the TM next to the aisle (seat H), before spreading towards the sides above the floor. After that, the fresh air is distributed in the complete row. The two other images Figure 3b) and c) present the flow structure for "C-1" with only 50% of the heat loads. For the "Norm Flow" case C-1.2 (Figure 3b), with increased T_{in} see Table 1), short-circuit currents were observed laterally under the luggage compartments. Thus, the visualizations confirm what was already suspected based on the outflow temperature. We found that a smaller force of inertial affects in depth of penetration. As a result, the fresh air is conveyed more poorly to the passengers. With reduced volume flow for C-1.1 in Figure 3c), the depth of penetration of the fresh air decreases even more.

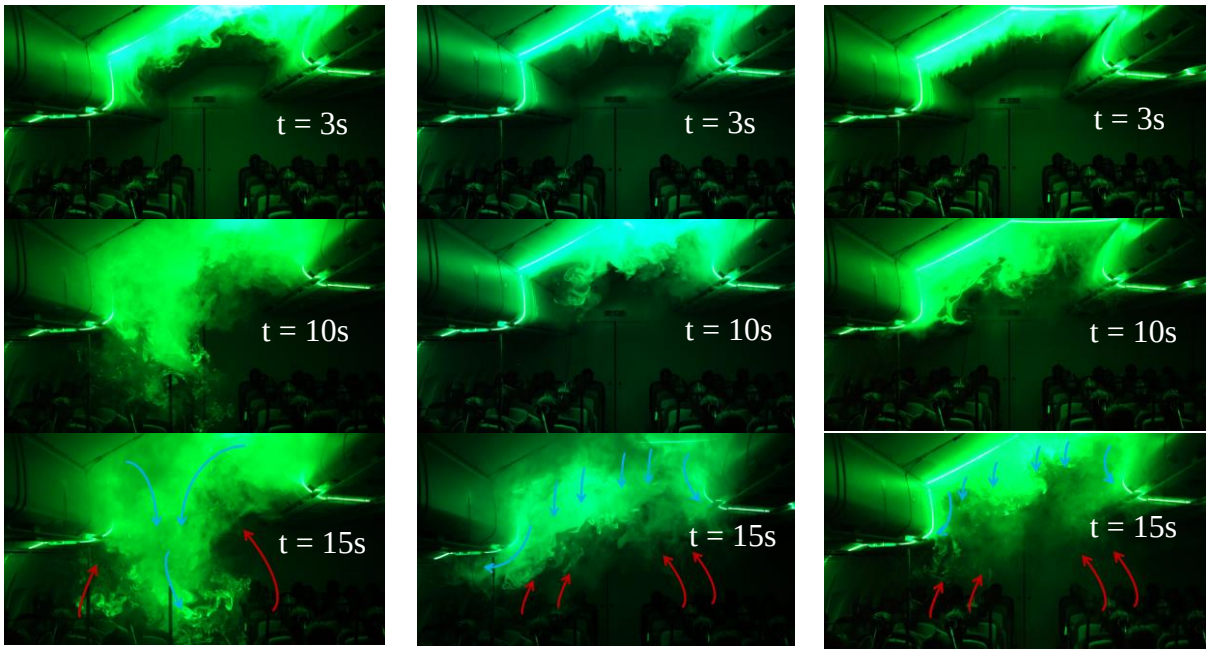

a) b) c)

Figure 3. Laser flow visualization in the aisle at MP 1 for a) reference case C-0, b) for case C-1.2 and c) for case C-1.1.

Figure 4 shows the temperature difference with respect to case 0 on chest level with regard to the fully occupied cabin over 1800 s in the vicinity of the TMs as contour plot from above. Thus, compared to C-0, red parts show the warmer temperatures and blue parts colder areas. For all cases, the missing heat loads were clearly visible as colder regions, see checkerboard pattern in Figure 4 a) and d), the unoccupied middle seats in b) and e) as well as the randomly chosen agglomeration of missing heat loads around rows 4 and 5 and seats G to K, in Figure 4 c) and f). Furthermore, as observed before, the seat arrangement has a significant impact on the temperature distribution. In spite of 50 missing passengers of case 1, almost all measured values are lower than the one the reference case 0. Obviously, a missing heat load does not have a major impact on this chest temperature. However, a temperature increase of up to 2.0 K could be observed for the occupied and adjacent seats. Switching to C-2 in Figure 4 b) and e) shows a greater influence with a temperature descent below the temperature of case 0 for the seats of the missing heat loads. Apart from individual places, the missing heat loads have

no major effect on the rest of the cabin. Both C-3 cases reveal the lowest overall temperatures, i.e. the highest negative deviations from the fully occupied cabin. Apparently, a group of missing heat loads has a greater impact on the entire cabin. With values up to 2.8 K, the largest differences between maximum and minimum temperature was found for both C-1 cases related to all switched-on as well as switched-off TMs, see Table 1. For case 2 in b) and e), we found a comparable maximum $\Delta\langle T_{Chest}\rangle$ of 2.9 K. With 1.9 K, the lowest and therefore the best result was observed for C-3. The spatial averaged standard deviations ($\sigma\langle T_{Chest}\rangle$) in Table 1 did not reveal any differences between the individual cases. A comparison of "Norm Flow" and "Adapted Flow" shows no major temperature differences. Hence, a reduction of the volume flow rate, which can result in a saving of energy, does not change the temperatures at chest level.

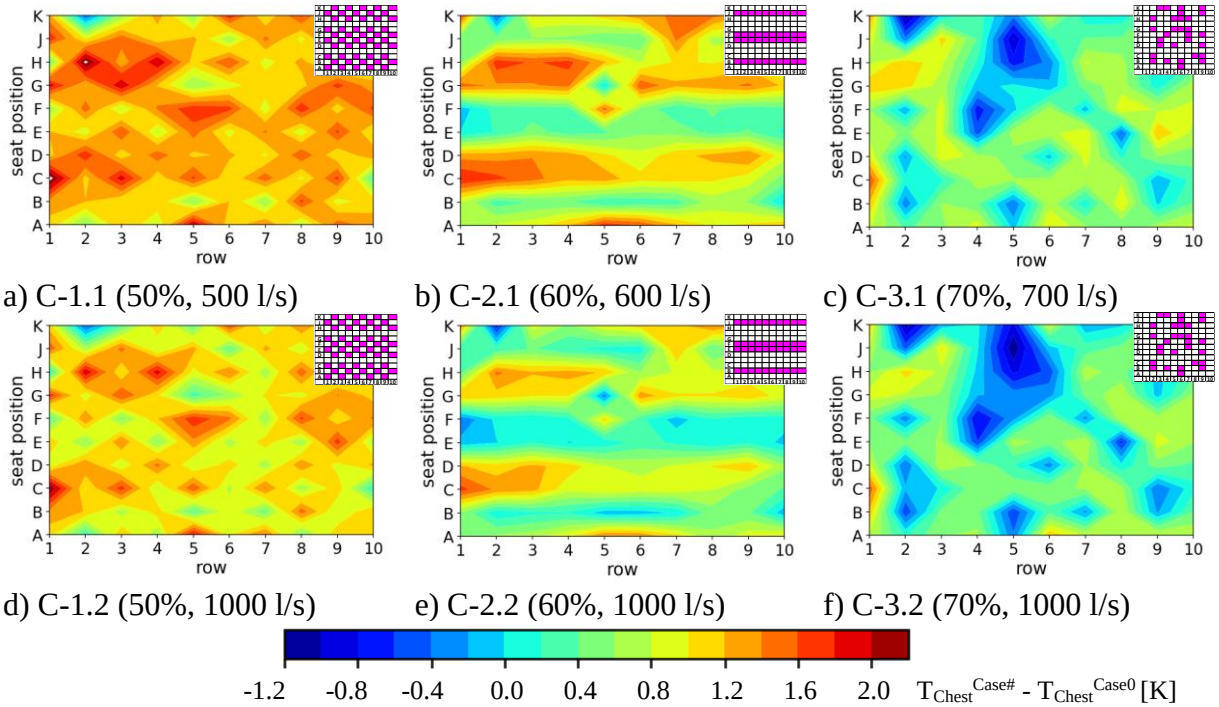

Figure 4. Contour plots of fluid temperature differences at chest position for a) C-1.2, b) C-2.2, c) C-3.2, d) C-1.1, e) C-2.1 and f) C-3.1. C.0 was deducted from all cases.

In the next step, ΔT_{cab} for all investigated cases under LMCV is discussed. Figure 5 (left) shows the mean temperature differences in the vicinity of the TMs averaged over 1800 s at four height levels (ankle, knee, chest, head) and ten positions of C-2.1 in row 4. Contrary to our expectations, the effect of the missing heat loads has no influence on the temperature on the occupied places. The lowest temperature difference was observed at the ankle for all cases. At knee position we found no major changes, the measured temperatures are almost identical to T_{cab}. In contrast to the falling values at ankle height, the temperatures at the upper body rise with a high number of missing heat loads due to the increased T_{in}, not pointed out here due to the lack of space. This results in a rising temperature different between head and ankle (ΔT_{HA}) only for the switched-on TMs from 5.2 K for C-0 to a maximum of 9.2 K for C-1.1, see Table 1. For the evaluation of the investigated cases, ΔT_{HA} is pivotal and rated as good for values less than 2.0 K as well as bad for temperature differences larger than 4.0 K, see Dehne et al. (2022). Furthermore, the standard deviations in Table 1 show a very good result after ASHRAE (2001) with values lower than 0.11 K for all temperatures.

For a deeper analysis of the impact of non-occupied seats on the thermal comfort, the values on four height levels for a time period of 1800 s but differentiated in switched-on and

switched-off TMs are shown for all cases in the boxplot in Figure 5 (right). Here, the rectangle with the orange median shows 50% of all measured values on 10 seats and four height levels. Furthermore, the whiskers reveal the complete range of data with outliers marked as circles.
The first thing to note is that the temperature differences range of the switched-off TMs is always below the switched-on TMs. However, the difference is very small. For all cases except of C-3, differences between “Norm Flow” and “Adapted Flow” were found. Here, we found a higher spreading of the data with “Adapted Flow”. As compared to C-0, the temperature range in the vicinity of switched-on as well as switched-off TMs increases with the amount of switched off TMs.

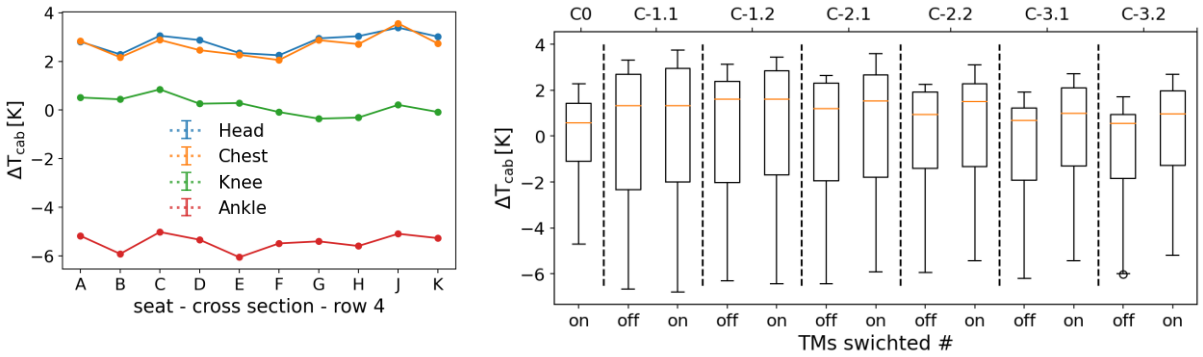

Figure 5. Left, mean temperature differences on four different height levels in the vicinity of the TMs, exemplarily shown for case C-2.1 and right, boxplot for the temperature differences in the vicinity of the thermal manikins on four different height levels for all investigated cases divided into switched on / off TMs

In addition to the local flow temperatures, the flow velocities in the passenger zone are an important criterion to evaluate passenger thermal comfort. Therefore, Figure 6 shows the fluid velocities averaged for a time period of 1800 s in row 6 at four height levels as boxplot just like the evaluation of fluid temperatures. With regard to the mean velocities, good results were observed on all measurement positions and all cases except for case C-0, maximum mean velocity of 0.31 m/s (red dashed line in Figure 6) which are one third of the value required as upper comfort threshold in ASHRAE (2001). However, the range of data (i.e. upper end of the whisker) for C-0 reveals values above this limit. Further, the case C-0 revealed many outliers, which were not observed on the occupied seats for all cases with missing heat loads. Despite the unchanged volume flow, the velocities are greatly reduced due to a lower number of heat loads. Just like in the study of the temperature, differences between “Norm Flow” and “Adapted Flow” were found for all cases except for case C-3. For this case even no major differences between switched-off and switched-on TMs were found, despite a different amount of outliers. In contrast to C-3, for the cases C-1 and C-2 reduced velocities were observed for the switched-off seats. Compared to the switched-on TMs, less distributed velocities, however, with a higher number of outliers, were observed for all switched-off cases, reflected by smaller boxes and shorter whiskers in Figure 6. Unlike the temperatures, the missing heat loads can be detected in the velocities, especially in C-1 and C-2. One reason for this is the lack of free convection, and thus, of buoyancy forces due to the missing heat loads.

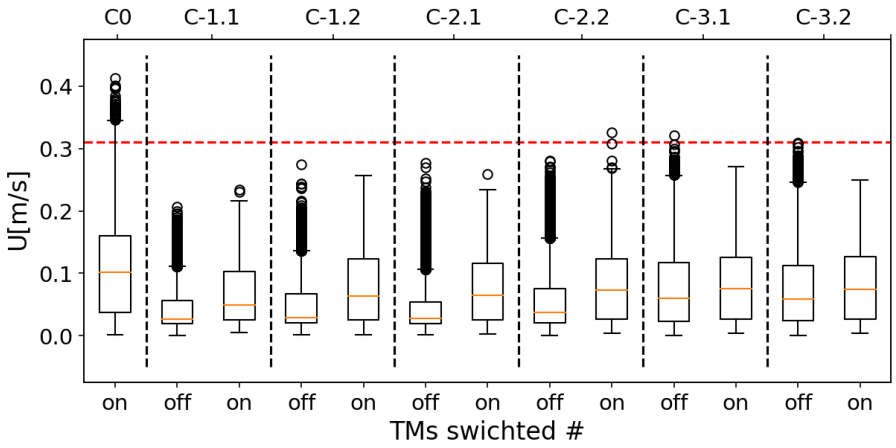

Figure 6. Boxplot for the velocities in the vicinity of the thermal manikins on four different height levels for all investigated cases divided into switched on / off TMs

4 CONCLUSIONS

In this study, we present the effect of missing heat loads on the temperature distribution in a full-scale twin aisle aircraft cabin mock-up. Three cases, each with "Norm" and "Adapted" volume flow rate, were compared to the fully occupied cabin using a novel, low-momentum ceiling ventilation (LMCV) air supply through planar and large-surface inlets. In summary, there are no major differences related to the thermal comfort between "Norm Flow" and "Adapted Flow" to the missing heat loads. This results in a saving of energy by reduced volume flow while maintaining thermal comfort. However, short-circuit currents were observed whereby a lot of fresh air leaves the cabin directly through the lateral outlets. Due to the buoyancy force, the fresh air is not flowing to the floor and cannot be used to cool the passengers. With a reduced volume flow due to a smaller number of passengers the depth of penetration of the fresh air decreases even more. Furthermore, the lack of heat loads leads to an increase of the temperature difference between head and ankle and thus potentially leads to discomfort. This can possibly be reduced by switching to a multi-zonal control, well known from previous studies. In the pursuing course of the project, the cases with missing heat loads will be compared with the reference case mixing ventilation as well as other novel systems.

ACKNOWLEDGEMENT

This project has received funding from the Clean Sky 2 Joint Undertaking under the European Union's Horizon 2020 research and innovation programme under grant agreement No. 755596. The responsibility of the content is the authors.

6 REFERENCES

ASHRAE. *ASHRAE Handbook of Fundamentals* Atlanta: ASHRAE, 2001
Bosbach et al., *CEAS Aeronautical Journal* 4, 301- 313, 2013
Bosbach et al., *ICAS2012*, Brisbane, Australia, September 23-28, 2012, ISBN 978-0-9565333-1-9
Dehne et al., *Roomventilation*, Espoo, Finland, June 2-5, 2018 #ID172
Dehne et al., *Ventilation Conference*, June 2022
EN 13129:2016, *Railways Application; Air Conditioning for Main Line Rolling Stock*, 2016
EN ISO 7730, *Ergonomics of the thermal environment*, Bruxelles, 2005.
IATA - International Air Transport Association, A global approach to reducing aviation emissions, 2009.
Lange et al., *AEC2020*, Bordeaux 25.-28. February 2020
Lange et al., *Indoor Air Conference*, submitted in January 2022
Martinez, *Aircraft Environmental Control*, P.U.o. Madrid, Madrid, Spain, 2014.
Schmidt, *Technical University of Denmark*, 2008
Yin et al., *Building Simulation*, 1030-1036, 2009
Zhang et al., *Building and Environment 42*, 1675-1684 (2007)